Contractility-dependent actin dynamics in cardiomyocyte sarcomeres

Aneta Skwarek-Maruszewska, Pirta Hotulainen, Pieta K. Mattila and Pekka Lappalainen*

Institute of Biotechnology, PO Box 56, 00014, University of Helsinki, Finland

*Author for correspondence (e-mail: pekka.lappalainen@helsinki.fi)

Accepted 3 March 2009
Journal of Cell Science 122, 2119-2126 Published by The Company of Biologists 2009
doi:10.1242/jcs.046805

Summary

In contrast to the highly dynamic actin cytoskeleton in non-muscle cells, actin filaments in muscle sarcomeres are thought to be relatively stable and undergo dynamics only at their ends. However, many proteins that promote rapid actin dynamics are also expressed in striated muscles. We show that a subset of actin filaments in cardiomyocyte sarcomeres displays rapid turnover. Importantly, we found that turnover of these filaments depends on contractility of the cardiomyocytes. Studies using an actin-polymerization inhibitor suggest that the pool of dynamic actin filaments is composed of filaments that do not contribute to contractility. Furthermore, we provide evidence that ADF/cofilins, together with myosin-induced contractility, are required to disassemble non-productive filaments in developing cardiomyocytes. These data indicate that an excess of actin filaments is produced during sarcomere assembly, and that contractility is applied to recognize non-productive filaments that are subsequently destined for depolymerization. Consequently, contractility-induced actin dynamics plays an important role in sarcomere maturation.

Supplementary material available online at
http://jcs.biologists.org/cgi/content/full/122/12/2119/DC1

Key words: ADF/cofilin, Actin, Contractility, Dynamics, Sarcomere

Introduction

The actin cytoskeleton has an important role in a number of motile and morphogenetic processes in non-muscle cells. Precisely, coordinated polymerization of actin filaments towards the plasma membrane pushes the leading edge forward and induces cell migration or elongation (Pantaloni et al., 2001; Pollard and Borisy, 2003; Chhabra and Higgs, 2007). Rapid actin dynamics play a central role also in the formation of plasma membrane invaginations during endocytosis and phagocytosis (Kaksonen et al., 2006). During these processes, actin assembly is regulated by a large number of proteins that control actin filament nucleation and polymerization (Pantaloni et al., 2001; Chhabra and Higgs, 2007; Paavilainen et al., 2004). The rapid actin polymerization is balanced by ADF/cofilin-induced disassembly of aged actin filaments away from the plasma membrane (Okreglak and Drubin, 2007).

In muscle cells, actin and myosin filaments, together with a large number of scaffolding and regulatory proteins, are arranged into regular contractile units, sarcomeres. These contractile structures are derived from stress-fiber-like premyofibrils at the edges of muscles cells. Premyofibrils gradually gain a more regular appearance and finally maturate to myofibrils that display highly regular sarcomeric organization (Sanger et al., 2005). The barbed and pointed ends of actin filaments in sarcomeres are capped by CapZ and tropomodulin, respectively (Casella et al., 1987; Schafer et al., 1995; Weber et al., 1994). In vertebrates, the lengths of actin filaments in sarcomeres are regulated by nebulin, which is a giant filamentous protein extending along the entire length of the thin filament. The C-terminus of nebulin is located at the Z-disc where it interacts with CapZ, α-actinin and myopalladin, whereas its N-terminus extends to the middle of the sarcomere where it interacts with tropomodulin (Gregorio et al., 1995; Littlefield et al., 2001; McElhinny et al., 2005; Witt et al., 2006; Bang et al., 2006; Pappas et al., 2008).

In contrast to most actin filament structures in non-muscle cells, the actin filaments in muscle sarcomeres are believed to be relatively stable. In muscle cells, GFP-actin and microinjected Rhodamine-labeled actin is incorporated mainly to the Z-discs and to the middle of the sarcomere (A-band region). This suggests that the turnover of the entire thin filament is likely to be very slow, but that the exchange of actin monomers at filament barbed and pointed ends regulates the length of thin filaments (Littlefield et al., 2001; Bai et al., 2007). However, fluorescence-recovery-after-photobleaching (FRAP) analyses suggested that also the entire thin filaments undergo turnover, although these studies provided highly variable turnover rates ($t_{1/2}$ ranging from several minutes to hours) (Suzuki et al., 1998; Hasebe-Kishi and Shimada, 2000; Wang et al., 2005). Despite the predicted slow turnover rates, two ADF/cofilin isoforms, which are proteins that promote rapid actin dynamics in other cell types (Carlier et al., 1997; Lappalainen and Drubin, 1997), are expressed in developing and adult striated muscles in mammals (Ono et al., 1994; Vartiainen et al., 2002). Point mutation in cofilin 2, which is the most abundant ADF/cofilin isoform in mature striated muscles, was shown to cause nemaline myopathy (Agrawal et al., 2007). Furthermore, muscle cells express a specific actin-nucleating protein, leiomodin, which localizes to the M-band region and is important for correct actin filament organization at least in cardiomyocyte sarcomeres (Chereau et al., 2008). These data indicate that actin filaments in muscle sarcomeres may be more dynamic than previously suggested.

Here, we examined the turnover of actin filaments in sarcomeres of neonatal rat cardiomyocytes. Interestingly, our analysis revealed that whereas the sarcomeric actin filaments in non-contractile cardiomyocytes are relatively stable, a subset of actin filaments in sarcomeres of actively contracting cells undergo rapid turnover. Furthermore, we provide evidence that the dynamic actin filament population in sarcomeres is composed of filaments that do not

contribute to contractility and show that contractility plays an important role in correct organization of actin filaments during sarcomere maturation.

Results

Actin filaments in cardiomyocyte sarcomeres display rapid contractility-dependent dynamics

Neonatal rat cardiomyocytes have regular, contractile myofibrils and are thus a good model for studying actin dynamics in striated muscles. To examine the kinetics of sarcomeric actin dynamics in live cells, we first used GFP-fusion of β-actin as a general tool to probe the rate of actin filament turnover in these cells. This construct has been widely applied as a marker for studying actin dynamics in various other systems, such as lamellipodia, filopodia and stress fibers of motile cells as well as in dendritic spines of neurons and sensory hair cell stereocilia (e.g. Koestler et al., 2008; Vignjevic et al., 2006; Hotulainen and Lappalainen, 2006; Colicos et al., 2001; Rzadzinska et al., 2004). In cardiomyocytes, the β-actin fusion protein was localized to sarcomeric actin structures, displaying a spatial distribution similar to that of Rhodamine-phalloidin-stained F-actin in these cells (supplementary material Fig. S1). Only the cells expressing low to moderate amounts of GFP–β-actin and with intact myofibrils were selected for further analysis. Thus, in these experiments a small amount of GFP–β-actin was incorporated into sarcomeric actin filaments, where it functioned as a probe to examine the dynamics of an entire filament that is mainly composed of endogenous actin subunits.

After isolation and plating on fibronectin for 3 days, 95% of the cardiomyocytes (both transfected and untransfected) displayed regular beating. FRAP analysis of several (more than ten) non-beating cells expressing GFP–β-actin revealed no detectable fluorescence recovery during the first 3 minutes after photobleaching (Fig. 1A), and only a weak fluorescence recovery during longer observation periods (data not shown). Although in the non-beating cells often the sarcomeric actin was less organized than in beating cells, these cells were viable and stained with the muscle α-actinin antibody, demonstrating that the regular actin arrays in these cells are indeed myofibrils (data not shown). Surprisingly, FRAP analysis of spontaneously beating cells expressing GFP–β-actin revealed relatively fast fluorescence recovery during the initial observation period (Fig. 1B). Analysis of the recovery profiles of >100 beating cells showed fast- ($t_{1/2}$ ~60 seconds) and slow ($t_{1/2}$ >30 minutes)-recovering populations of actin arrays consisting of 20-30% and 70-80% of total actin in sarcomeres, respectively (Fig. 1D; and data not shown).

To examine whether the lack of actin dynamics in non-beating cells indeed results from the lack of contractility, we treated cardiomyocytes with 2,3-butanedione monoxime (BDM). Although BDM is a relatively non-specific myosin II inhibitor, it can be used to inhibit the contractility of cardiomyocytes. Furthermore, BDM does not affect cell viability because the treatment was reversible, and the cardiomyocytes began to beat after washout of the compound (data not shown). Fig. 1C shows a FRAP analysis of a beating cell expressing GFP–β-actin. Before BDM treatment, approximately 30% of sarcomeric actin was rapidly turning over. However, in FRAP analysis repeated after BDM treatment, when the cell had stopped beating, only weak recovery (<10%) was detected during the observation period (Fig. 1C,D).

Because BDM is a relatively non-specific myosin inhibitor and appears to perturb actin nucleation in fibroblasts through mis-targeting of the Arp2/3 complex (Yarrow et al., 2003), we also

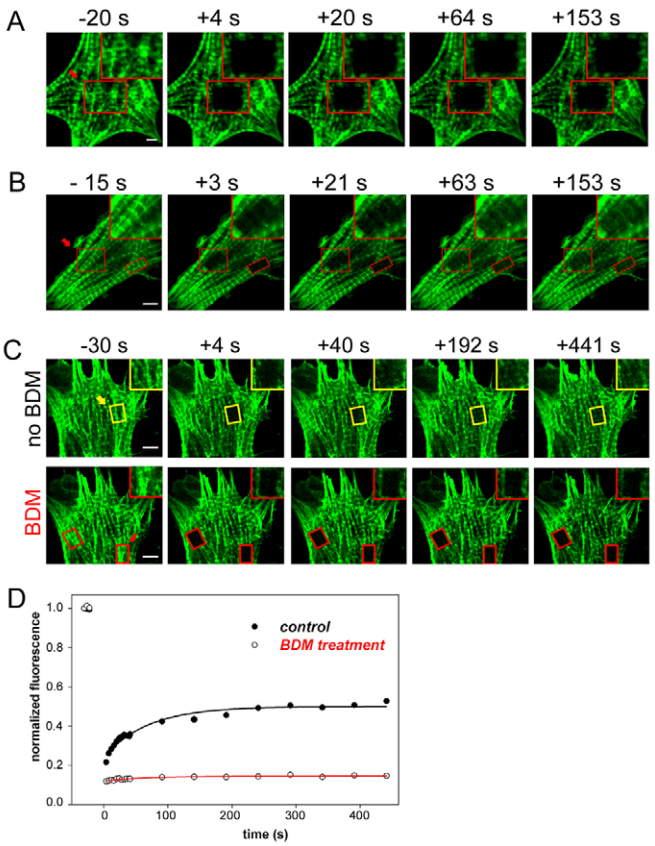

Fig. 1. Actin dynamics in cardiomyocyte sarcomeres is dependent on contractility. Selected regions were photobleached from non-beating (A) and spontaneously beating (B) cardiomyocytes expressing GFP–β-actin. Time-lapse sequences before (–20 s) and immediately after (+4 s) photobleaching are shown together with selected time-lapse frames. Arrowheads indicate the photobleached area that is shown in higher magnification in insets. Sarcomeric actin in beating cells is rapidly turned over, whereas only very weak fluorescence recovery of GFP–β-actin was detected in non-beating cells during the observation period. Note that sarcomeres are often more disorganized in non-beating cells. (C) Time-lapse images of fluorescence recovery of spontaneously beating cardiomyocyte before (upper panel) and 10 minutes after BDM (2,3 butanedione monoxime) treatment (lower panel). There was rapid actin turnover in the sarcomeric structures of the cell before treatment. However, after inhibition of beating by BDM, no fluorescence recovery in photobleached regions was observed. Scale bars: 5 μm. (D) Recovery profile of bleached zone over the time course of the FRAP experiment. Before BDM treatment, there was rapid turnover of approximately 30% of GFP–β-actin, whereas inhibition of beating by BDM treatment halts actin turnover. The experiments were performed in cells cultured for 2 days.

examined the role of contractility in cardiomyocyte actin dynamics by using a more specific myosin inhibitor, blebbistatin (Straight et al., 2003). Blebbistatin was reported to be labile and phototoxic when exposed to light with a wavelength of <490 nm (Kolega, 2004), and thus the FRAP experiments in the presence of blebbistatin were carried out on cells expressing mCherry–β-actin and using an excitation wavelength of 561 nm. mCherry–β-actin localized to myofibrils in neonatal cardiomyocytes similarly to GFP–β-actin. In FRAP experiments, approximately 30% of mCherry–β-actin in the sarcomeres of contractile cells displayed rapid dynamics. Importantly, inhibition of contractility by blebbistatin diminished the size of the dynamic actin filament pool similarly to BDM (Fig. 2). It is important to note, that GFP and mCherry alone had a predominantly diffuse cytoplasmic localization

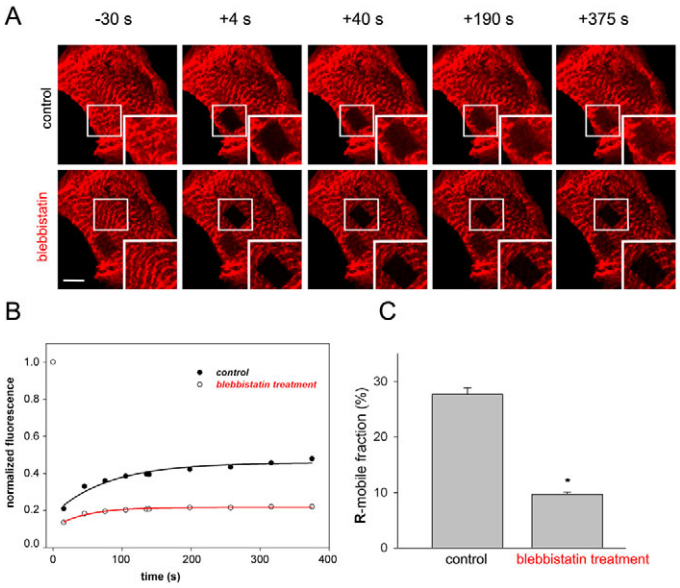

Fig. 2. Inhibition of contractility by blebbistatin diminishes the size of the dynamic actin filament pool in cardiomyocytes. (A) Time-lapse images of fluorescence recovery of spontaneously beating cardiomyocyte before (upper panel) and 10 minutes after blebbistatin treatment (lower panel). A population of sarcomeric actin filaments showed rapid actin turnover before treatment. However, after inhibition of beating by blebbistatin, only very weak fluorescence recovery of photobleached regions occurred. Scale bars: 5 µm. (B) Recovery profile of the bleached zone over the time course of the FRAP experiment. (C) Quantification of the dynamic actin pool from nine cells before and four cells after blebbistatin treatment. Before blebbistatin treatment, approximately 30% of mCherry–β-actin was rapidly turning over, whereas after blebbistatin treatment the size of the dynamic actin pool was approximately 10%. The cells were cultured for 2 days before experiments. The error bars indicate s.e.m. *Statistically significant at $P<0.0001$.

in cardiomyocytes and that their dynamics were not affected by BDM or blebbistatin treatments (supplementary material Fig. S2). Together, these data show that cardiomyocyte sarcomeres are composed of dynamic and non-dynamic actin filament populations, and that the turnover of the dynamic population is dependent on contractility.

Six actin isoforms are found in vertebrates. The predominant isoform expressed in the adult heart is α-cardiac actin (Chaponnier and Gabbiani, 2004). Western blot analysis using antibodies specific to β-actin and α-cardiac actin demonstrated that whereas α-cardiac actin is expressed at relatively high levels in cultured cardiomyocytes, only very low amounts of β-actin are expressed in these cells. Furthermore, whereas the levels of α-cardiac actin stayed constant during the period of 1-5 days after isolation, the levels of β-actin decreased during cardiomyocyte maturation (Fig. 3A). Although both actin fusion proteins localized to the sarcomeric actin structures, with a spatial distribution similar to that of Rhodamine-phalloidin-stained F-actin in these cells, immunofluorescence microscopy revealed that only a subset (>10%) of cardiomyocytes expressed detectable amounts of β-actin (Fig. 3B; supplementary material Fig. S1; and data not shown). For these reasons, it was important also to examine dynamics of the major isoform, cardiac-α-actin, in cardiomyocyte sarcomeres.

Similarly to GFP–β-actin, there was rapid turnover of GFP–α-cardiac actin in beating cells (Fig. 3B,C), whereas this turnover was not observed in spontaneously non-beating cells or cells treated with BDM (supplementary material Fig. S3). The population of α-cardiac actin filaments (~25% at day 2 after isolation) that displayed rapid actin dynamics was slightly smaller than the population of β-actin filaments (~32% at day 2). Furthermore, populations of the dynamic actin filaments diminished during maturation of both isoforms (Fig. 3C). The rate of fluorescence recovery was not dependent on the actin isoform or the maturation stage of cardiomyocytes, because the $t_{1/2}$ of the fluorescence recovery for both actin isoforms was approximately 60 seconds in the sarcomeres of cardiomyocytes from 2 to 4 days after isolation. The relatively small differences between the $t_{1/2}$ values are most probably within the range of experimental error (supplementary material Fig. S4). Together, these assays show that sarcomeric actin filaments in cardiomyocytes undergo contractility-dependent turnover and that this dynamics is not a specific feature of a certain actin isoform.

The dynamic actin filament population is composed of filaments that do not contribute to contractility

Previous studies carried out by microinjecting Rhodamine-labeled actin into cardiomyocytes and by expressing GFP-actin in *Drosophila* muscles suggested that only the ends of actin filaments are dynamic in striated muscle cells (Littlefield et al., 2001; Bai et al., 2007). However, in our experiments using contractile cardiomyocytes we did not observe fast fluorescence recovery from either the M-band or Z-disc regions. Instead, the recovery profiles of GFP-actin resembled the original sarcomeric actin intensity profiles recorded before photobleaching (Fig. 4). This observation provides evidence that the contractility-dependent dynamic actin pool in cardiomyocytes is indeed composed of sarcomeric actin filaments and not of non-sarcomeric actin structures. Furthermore, these data suggest that contractility-induced actin dynamics in sarcomeres is a stochastic process, during which individual filaments are depolymerized and non-synchronously replaced by new actin filaments.

To reveal whether the dynamic actin filament population is composed of correctly aligned filaments that contribute to contractility, or of filaments that are not necessary for contraction, 3-day-old cardiomyocytes were treated with actin polymerization inhibitor, latrunculin B. This drug does not actively depolymerize actin filaments, but instead disassembles the dynamic actin filament pool by sequestering actin monomers. Thus, at short incubation times, latrunculin B is expected to deplete the most dynamic actin filaments while the stable actin filaments should stay intact (Coue et al., 1987; Ayscough et al., 1997). In cardiomyocytes, short (10-30 minute) latrunculin B treatment should promote the disassembly of dynamic non-sarcomeric actin filament structures as well as deplete the dynamic sarcomeric actin filament pool identified above in Figs 1-4. It is important to note that a previous study suggested that myofibrils are stable in the presence of latrunculin A, but did not address the possible effects of this compound on sarcomere morphology and contractility (Wang et al., 2005).

After depolymerization of the dynamic actin filament pool by treatment for 10-30 minutes with latrunculin B, sarcomeric actin structures became more regular, characterized by wider and more visible M-bands (Fig. 5A). Latrunculin-B-treated cells also had less F-actin staining outside the actual sarcomeric structures, suggesting that the non-sarcomeric actin structures undergo relatively rapid turnover. FRAP analysis of GFP–β-actin-expressing cells demonstrated that the majority of the dynamic actin pool in myofibrils was depleted after latrunculin B treatment (Fig. 5B). Importantly, latrunculin B treatment did not affect the number of

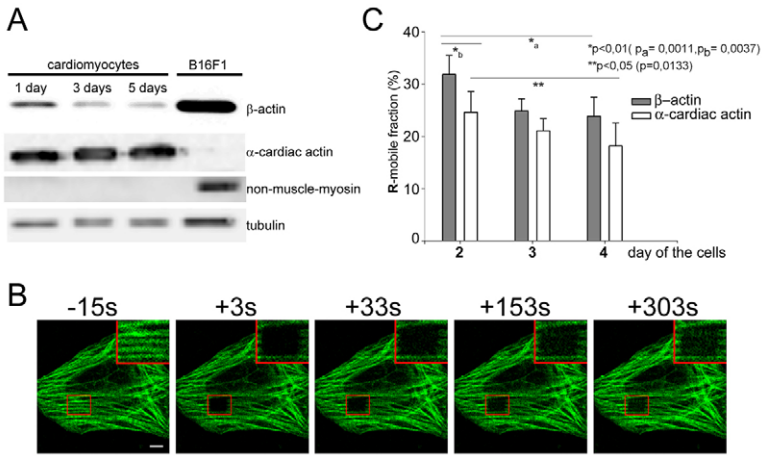

Fig. 3. The size of the dynamic actin filament pool is dependent on the actin isoform and age of the cardiomyocytes. (A) A western blot analysis demonstrating that β-actin and α-cardiac actin are coexpressed in cardiomyocytes. However, the levels of β-actin decrease during cardiomyocyte maturation, whereas the amount of α-cardiac actin stayed constant. The amount of β-actin in muscle cells was much lower than in the B16F1 non-muscle cell line. Equal amounts of the cell lysates (10 µg) were used for western blotting. The blots were also probed with non-muscle myosin antibody to evaluate possible fibroblast contamination of cell lysates, and tubulin antibody was used as a loading control. (B) Actin dynamics in a beating cardiomyocyte expressing GFP–α-cardiac actin was measured by FRAP. Similarly to β-actin, contractility-dependent turnover of α-cardiac-actin filaments also occurred. Scale bar: 5 µm. (C) The sizes of mobile β-actin and α-cardiac actin pools decreased during cardiomyocyte maturation. Furthermore, the size of dynamic actin filament pool was approximately 25% smaller for α-cardiac actin as compared with β-actin. Error bars indicate s.e.m.; on day 2, n=22, n=17 for β-actin and α-cardiac actin, respectively, and on day 4, n=14, n=12 for β-actin and α-cardiac actin, respectively.

spontaneously beating cells (Fig. 5C). However, the beating of latrunculin-B-treated cells was less synchronous as compared to non-treated cells, suggesting that gap junctions or intercalated discs in cardiomyocytes may depend on the dynamic non-sarcomeric actin structures (supplementary material Movies 1 and 2). Collectively, these results suggest that contractility-dependent actin turnover induces depolymerization of non-productive actin filaments in cardiomyocyte myofibrils, whereas the correctly aligned sarcomeric actin filaments, contributing to contractility, are significantly more stable.

Proper assembly of actin filaments in cardiomyocyte sarcomeres depends on contractility

By examining the organization of sarcomeric actin arrays of cardiomyocytes at different time points after isolation and plating on fibronectin, we noticed that re-formation of myofibrils is accompanied with a dramatic change in the organization of sarcomeric actin structures. After isolation and plating, F-actin staining of the myofibrils was uniform, without visible lack of F-actin in the M-band region. However, the Z-discs were nearly formed, as seen by the striated pattern of muscle α-actinin. Between 24 and 44 hours after plating, the cells began to beat, and this was accompanied by the appearance of regular sarcomeres with a lack of visible F-actin staining at the M-band (Fig. 6A). Furthermore, tropomodulin had a relatively diffuse distribution pattern in newly plated cardiomyocytes, whereas this filament-pointed-end capping protein concentrated at M-band regions in well-organized sarcomeres of contractile cells (supplementary material Fig. S5).

It was previously reported that inhibition of myosin activity by BTS (*N*-benzyl-*p*-toluene sulphonamide) and BDM, suppressed the organization of actin and myosin into cross-striated structures in primary cultures of chick embryonic skeletal muscle (Soeno et al., 1999; Kagawa et al., 2006). Furthermore, myofibril assembly can be accelerated by electric pulse stimulation in cultured C2C12 cells (Fujita et al., 2007). To confirm that contractility is also important for the proper assembly of myofibrils in neonatal cardiomyocytes, we inhibited contractility 24 hours after plating with blebbistatin

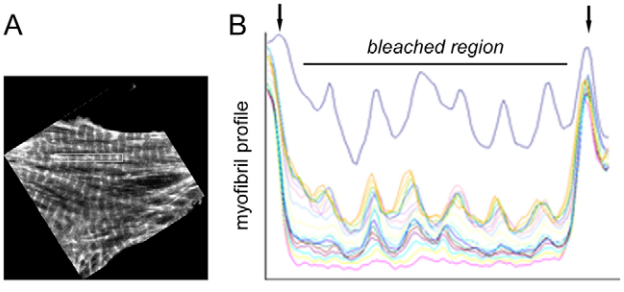

Fig. 4. Fluorescence recovery profile of sarcomeres. (A) Horizontally rotated fragment of a beating cardiomyocyte expressing GFP–β-actin. The region where the recovery profile was analyzed is indicated by the white rectangle. (B) Recovery profile of the photobleached region followed in time. Upper (blue line) represents the fluorescence intensity before photobleaching and the other profiles indicate recovery profiles 4-321 seconds after bleaching. Arrows indicate non-bleached sarcomeres surrounding the photobleached region.

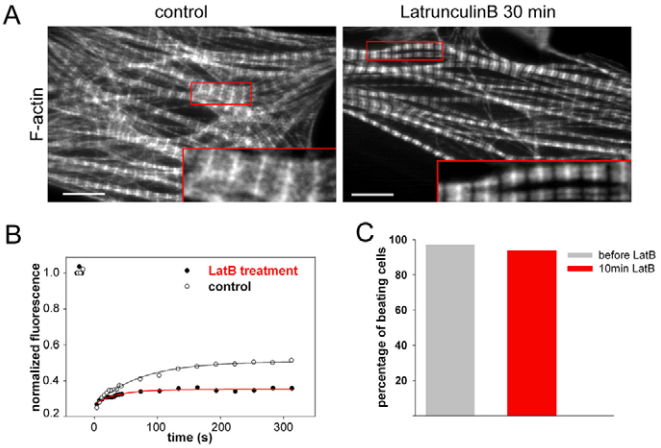

Fig. 5. The dynamic actin filament pool in sarcomeres is composed of misaligned filaments that do not contribute to the contractility. (A) Depolymerization of the dynamic filament pool by 20 µM latrunculin B for 30 minutes leads to a more regular appearance of sarcomeric actin structures (right panel) as compared with those of the control cell (left panel). Insets show selected regions of the cells (boxed) at higher magnification. F-actin was visualized by phalloidin staining. Scale bar: 10 µm. (B) Depolymerization of the dynamic actin filament pool by latrunculin B halts actin filament turnover in sarcomeres as determined by FRAP analysis from a representative GFP–β-actin-expressing cell before and after latrunculin B treatment. (C) Latrunculin B treatment does not halt beating of cardiomyocytes, demonstrating that the dynamic actin filament pool is not required for contractility (>100 cells from each group were analyzed for beating). The experiments were performed in cells cultured for 3 days.

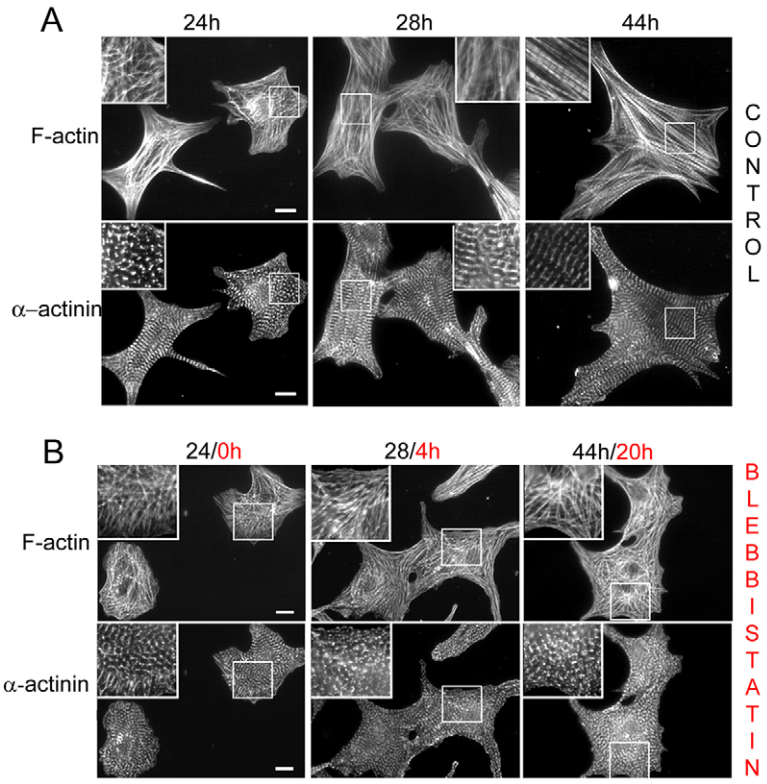

Fig. 6. Contractility is important for generation of regular sarcomeric actin arrays in cardiomyocytes. (A) 24 hours after plating, the myofibrils of cardiomyocytes have a uniform F-actin staining, whereas α-actinin already has a typical striated distribution pattern. Between 24 and 44 hours after plating, the cells began to beat and the F-actin staining of myofibrils became periodic, with a lack of F-actin at the M-band region. (B) When contractility of these cells was inhibited at 24 hours after plating with 100 µM blebbistatin, the maturation of the periodic F-actin pattern along myofibrils was prevented, as seen at the 28- and 44-hour time-points. Scale bar: 10 µm.

(Fig. 6B) or BDM (data not shown). Importantly, in the presence of these myosin inhibitors myofibrils failed to mature and did not develop the regular sarcomeric F-actin pattern. Also Z-disc organization was affected. Nevertheless, the cells were viable because they began to contract after BDM washout. These data show that the maturation of myofibrils is accompanied by a more regular appearance of sarcomeric actin filament arrays and that the reorganization of sarcomeric actin arrays during maturation is dependent on contractility.

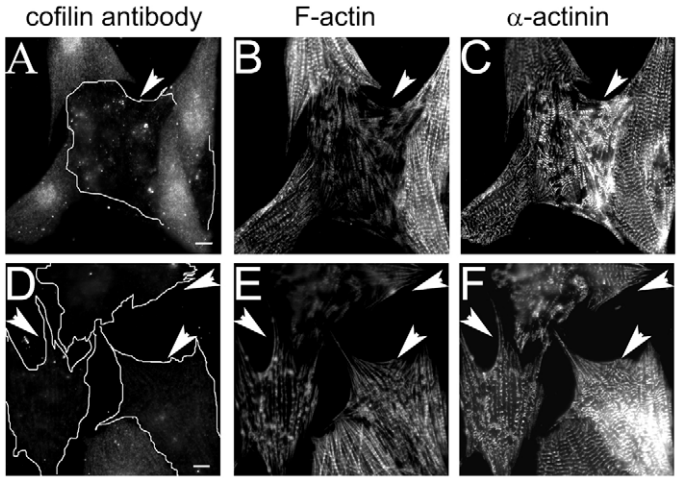

Fig. 7. ADF/cofilins are required for correct assembly of actin filaments in sarcomeres. (A,D) Cells transfected with Alexa-Fluor-488–cofilin 1 siRNA and Alexa-Fluor-488–cofilin 2 siRNA oligonucleotides had reduced staining of antibody to cofilin 1 and 2 (arrowheads). (B,E) Phalloidin staining of F-actin shows severely disorganized sarcomeric actin structures in cofilin-1 and cofilin-2 knockdown cells (arrowheads). (C,F) Sarcomeric α-actinin staining of Z-discs of cofilin-1 and cofilin-2 knockdown cells (arrowheads). The borders of the transfected cells are indicated by white lines. Scale bars: 10 µm.

ADF/cofilins are essential for correct organization of sarcomeric actin arrays

Two ADF/cofilin isoforms, cofilin 1 and cofilin 2, are expressed in striated muscles, cofilin 2 being the dominant isoform in mature muscles (Ono et al., 1994; Vartiainen et al., 2002). Cofilin 1 and cofilin 2 are ~80% identical at the amino acid level and no isoform-specific antibodies for these proteins are available. To evaluate whether ADF/cofilins promote actin dynamics in sarcomeres or if they only contribute to dynamics of non-sarcomeric actin structures in muscle cells, we depleted cofilin 1 and cofilin 2 simultaneously from cardiomyocytes by RNAi. The simultaneous transfection of cells with fluorescently labeled cofilin 1 and cofilin 2 oligonucleotides resulted in drastic decrease in the cellular levels of cofilin 1 and 2 as detected by western blotting (supplementary material Fig. S6A). Immunofluorescence microscopy with antibody to cofilin 1 and 2 revealed that the proportion of cells negative to cofilin 1 and 2 was ~50% (Fig. 7A,D). As compared to the non-transfected neighboring cells, the cofilin-1 and cofilin-2 knockdown cells typically had severely disorganized sarcomeric actin filaments (Fig. 7B,E) and a lack of beating and fluorescence recovery as determined from cells expressing GFP-actin (supplementary material Fig. S6B,C). In contrast to ADF/cofilin-depleted non-muscle cells (Hotulainen et al., 2005), depletion of ADF/cofilins from cardiomyocytes did not result in a clear increase in the amount of F-actin, and in some RNAi cells the amount of F-actin appeared to be diminished as compared to non-transfected neighboring cells (Fig. 7B,E). A possible explanation for this difference is that whereas in non-muscle cells the expression of actin genes is controlled by

free actin monomers through the MAL-SRF pathway, the muscle cell counterpart of MAL, myocardin, is not regulated by free actin monomers (Schratt et al., 2002; Vartiainen et al., 2007; Guettler et al., 2008).

Analysis of cells transfected only with oligonucleotides specific to either one of the isoforms suggested that depletion of cofilin 2 leads to more severely disorganized sarcomeric actin cytoskeleton than depletion of cofilin 1 (data not shown). However, because of a lack of specific antibodies that would recognize only cofilin 1 or cofilin 2 from rat cardiomyocytes, the relative importance of the two ADF/cofilin isoforms in the organization of cardiomyocyte sarcomeres cannot be reliably examined. Together, these results demonstrate that ADF/cofilins play an important role in the organization of actin filaments of myofibrils in mammalian striated muscle cells. In support of these data, it was shown that mutations in UNC-60B, the *C. elegans* homolog of ADF/cofilins, led to defects in actin organization in the body wall muscles in these worms (Ono et al., 1999).

Discussion

Although the turnover of entire actin filaments in myofibrils was reported to be slow and it has been suggested that in sarcomeres turnover occurs mainly at the filament ends to maintain correct thin filament length (Littlefield et al., 2001; Bai et al., 2007; Hasebe-Kishi and Shimada, 2000), many proteins that promote rapid actin dynamics in other cell types are also present in muscles (e.g. Ono et al., 1994; Vartiainen et al., 2002; Bertling et al., 2004; Yamashiro et al., 2008). This led us to examine the turnover of actin filaments in neonatal cardiomyocytes, which display regular sarcomeric actin arrays and undergo spontaneous beating (= contractility) in cell culture conditions. Surprisingly, analysis of GFP-actin and mCherry-actin dynamics in myofibrils of actively contracting and non-contractile cardiomyocytes revealed that a subset of actin filaments in sarcomeres undergoes rapid turnover that is dependent on contractility. Our FRAP experiments also provide evidence that during contractility-induced actin dynamics, entire actin filaments are replaced by new ones in sarcomeres. Furthermore, we show that cardiomyocyte maturation is accompanied by an increase in the regular organization of sarcomeric actin filaments and contractility-induced actin dynamics may thus play an important role in depolymerization of non-productive actin filaments during this process. Finally, RNAi studies revealed that, in addition to contractility, ADF/cofilins play a central role in dynamics and organization of actin filaments in cardiomyocyte sarcomeres. Together, these findings suggest that nucleation and polymerization of new actin filaments occurs during sarcomere maturation, and that only the correctly aligned filaments are protected against contractility-dependent depolymerization. In support to rapid actin filament nucleation and/or polymerization in muscle cells, a recent study identified a muscle-specific actin filament nucleator, leiomodin, which localizes to the M-band region in neonatal rat cardiomyocytes and plays an important role in organization of sarcomeric actin arrays (Chereau et al., 2008).

These and previous data by Littlefield et al. (Littlefield et al., 2001) suggest that sarcomeres undergo two types of actin dynamics: (1) contractility-dependent turnover of entire filaments, and (2) exchange of actin monomers at filament ends to maintain correct thin filament length. It is probable that the majority of thin filaments in sarcomeres undergo exchange of actin monomers at their ends, whereas only a subset of actin filaments undergo rapid contractility-dependent turnover. Thus, the former filament turnover type is expected to dominate in studies where incorporation of fluorescently labeled actin into myofibrils is examined after relatively long time periods [e.g. 1 hour in the study by Littlefield et al. (Littlefield et al., 2001)]. Correspondingly, in FRAP experiments, in which actin dynamics in myofibrils is examined in a shorter time-scale, the rapid contractility-dependent turnover of entire actin filaments is expected to dominate. The presence of two distinct types of actin dynamics in sarcomeres is also supported by inhibition of contractility-dependent actin dynamics in cardiomyocytes by cytochalasin D (A.S.-M. and P.L., unpublished), suggesting that contractility-dependent actin dynamics is driven by actin filament polymerization at barbed ends. Thus, our data, revealing both dynamic contractility-dependent and relatively stable actin populations in cardiomyocyte sarcomeres provides an explanation for previous and seemingly contradictory results concerning actin dynamics in muscle cells (Littlefield et al., 2001; Bai et al., 2007; Wang et al., 2005).

Although the exact nature of the dynamic actin filament pool in myofibrils is unknown, we propose that contractility-dependent actin dynamics contributes to sarcomere maturation and replacement of damaged actin filaments in fully mature muscles. In addition to correctly aligned filaments, immature sarcomeres appear to contain a significant amount of actin filaments that do not contribute to contractility. Our data also suggest that in 'mature' cardiomyocytes the population of non-productive filaments is smaller as compared to 'immature' cardiomyocytes. The sarcomeric actin filaments are very stable in non-contractile cells, whereas contractility induces rapid depolymerization of the non-productive filaments. These may be subsequently replaced by rapid actin filament nucleation at the M-band region by leiomodin (Chereau et al., 2008).

The rapid actin filament disassembly in sarcomeres of contractile cells may be promoted by several different mechanisms. Contractility may for example bend actin filaments that are not properly associated with the Z-disc or transport them to the M-band region. Alternatively, myosin II itself may induce filament depolymerization as recently demonstrated in vitro (Haviv et al., 2008). Thus, future studies are required to elucidate the exact mechanism of how contractility induces actin dynamics in myofibrils. Furthermore, determining the mechanism by which ADF/cofilins contribute to sarcomeric actin dynamics is an important challenge for future studies.

In the future it will be important to examine whether contractility-induced actin dynamics is limited to muscle maturation or if it also takes place after muscle injury, providing a partial explanation for why exercise (muscle contractility) is important for recovery after muscle injury. It is also important to note that myosin II activity was shown to promote actin dynamics during cytokinesis and in neuronal growth cones (Murthy and Wadsworth, 2005; Guha et al., 2005; Medeiros et al., 2006). Thus, contractility-dependent actin dynamics may play a more general role in the organization of different types of actin arrays in various cell-types.

Materials and Methods

Isolation of neonatal rat cardiomyocytes

Neonatal (day 1-3) rat (Wistar Han) hearts were dissected, cut into small pieces and digested with collagenase (0.5 mg/ml; Worthington Biochemical Corp.) and pancreatin (0.6 mg/ml; Gibco Laboratories). To deplete fibroblasts from the cell suspension, the cells were pre-plated in Dulbecco's modified Eagle's medium (DMEM) plus medium 199 (4:1) supplemented with 10% horse serum and 5% (heat inactivated) fetal bovine serum (FBS), 4 mM glutamine, 1% penicillin-streptomycin. Cardiomyocytes were then plated on fibronectin-coated (10 μg/ml; Sigma-Aldrich) plastic dishes (Nunc) and cultured in maintenance medium (20% medium M199, 75% DBSS-K, 4% horse serum, 4 mM glutamine, 1% penicillin-streptomycin, 0.1 mM phenylephrine; DBSS-K: 6.8 g/l NaCl, 0.14 mM NaH_2PO_4, 0.2 mM $CaCl_2$, 0.2 mM $MgSO_4$, 1 mM dextrose,

2.7 mM $NaHCO_3$). Using this method, >95% of the cells in the primary culture were cardiomyocytes. For live-cell imaging and FRAP experiments, cells were plated on fibronectin-coated glass-bottom culture dishes (MatTek) and treated as described above.

Immunofluorescence microscopy and western blotting

Cells were fixed for 20 minutes in 4% paraformaldehyde in PBS and permeabilized with 0.2% Triton X-100 in PBS for 7 minutes. Indirect immunofluorescence was carried out as previously described (Vartiainen et al., 2000) with the following antibodies and dilutions: anti-sarcomeric-α-actinin (clone EA 53, Sigma-Aldrich) 1:500, anti-tropomodulin 1:750 (a gift from Carol C. Gregorio, University of Arizona, Tuscon, AZ) and anti-cofilin 1:100 (Hotulainen et al., 2005). Specific IgGs were revealed with FITC or Cy5-conjugated secondary antibodies (Invitrogen) at 1:250 dilution. Actin filaments were visualized with Alexa Fluor 488 or Rhodamine-conjugated phalloidin diluted 1:300 (Molecular Probes, Invitrogen). Images were acquired as described previously (Hotulainen and Lappalainen, 2006). The cells for western blotting were treated as described previously (Hotulainen et al., 2005). For western blotting, anti-β-actin (clone AC-15, Sigma-Aldrich) was used at a dilution of 1:10.000, anti-α-cardiac actin (Acris) at a dilution of 1:1000, anti-nonmuscle-myosin (Biomedical Technologies) 1:600, anti-cofilin 1:1000 (Hotulainen et al., 2005) and anti-tubulin at 1:5.000 (Sigma-Aldrich). Latrunculin B was obtained from Molecular Probes.

siRNA treatment

For the siRNA experiments, 1500 ng of preannealed 3′ Alexa-Fluor-488-labeled cofilin-1 siRNA described by Bertling et al. (Bertling et al., 2004) and Alexa-Fluor-488-labeled cofilin-2 siRNA [r(GCAGUUCUCUUCUGUUUAA)d(TT), r(UUAAACAGAAGAGAACUGC)d(TT)] (Qiagen) oligonucleotide duplexes were co-transfected into the cardiomyocytes 1 day after isolation by using Gene Silencer's siRNA-transfection reagent (Gene Therapy Systems) according to manufacturer's recommendations. The levels of cofilin 1 and 2 were examined 24 hours after transfection by immunofluorescence and western blot analysis using antibodies described above. For live cell imaging, cells were first transfected with GFP–β-actin and 24 hours later co-transfected with a cofilin-1–cofilin-2 siRNA mixture.

Plasmid construction

Human GFP–β-actin plasmid (Choidas et al., 1998) and mCherry–β-actin plasmid were gifts form Martin Bähler (Westfalian Wilhelms University, Münster, Germany). A DNA fragment corresponding to the open reading frame of the mouse α-cardiac actin was amplified from mouse cDNA by using nucleotides that created *Xho*I and *Bam*HI sites at the 5′ and 3′ ends of the polymerase chain reaction (PCR) fragment, respectively. The fragment was digested and ligated to pEGFP-C1A to create plasmid GFP–α-cardiac actin. The sequence of the construct was verified by sequencing.

Fluorescence recovery after photobleaching and statistic analysis of FRAP data

The cells were transiently transfected with GFP and mCherry constructs 1 day after isolation using Escort III (Sigma-Aldrich) according to the manufacturer's specification and cultured in the maintenance medium. FRAP experiments were carried out as described previously (Hotulainen and Lappalainen, 2006). After photobleaching the fluorescence recovery was monitored ten times every 3.9 seconds and ten times every 30 seconds. Owing to extremely rapid fluorescence recovery in the control GFP and mCherry FRAP experiments, the recovery in these cases was monitored ten times every second and ten times every 3 seconds. The recovery of the GFP intensity was measured by Leica confocal software (LCS). The intensity of the bleached area was normalized to a neighboring non-bleached area to diminish error caused by normal photobleaching during the monitoring period. The data was fitted with curves using SigmaPlot graphical analysis software. The time course of recovery was fitted to the following single equation for a exponential: $y(t)=y_0+R(1-e^{-\tau t})$ where y_0 is an offset and R is a mobile fraction. Statistical significance (P-value) was determined using the Student's t-test. To generate a recovery profile the data was exported from LCS (Leica Microsystems) in avi format, merged to a single file in Imaris Pro 6.1 (Media Cybernetics), rotated 32° to get the area of interest horizontal, measured time-point by time-point with the thick horizontal line profile tool, and exported to and averaged in Microsoft Excel.

Inhibition of contraction by BDM and blebbistatin treatment

The cells were plated on 10 μg/ml fibronectin-coated dishes. Twenty-four hours after plating, 100 μM of blebbistatin in DMSO or DMSO alone (control) was added to the maintaining medium. The cells were incubated (37°C, 5% of CO_2) for a further 4 or 20 hours, fixed and immunostained. For FRAP experiments, 40 μM of BDM (Sigma-Aldrich) or 100 μM of blebbistatin (Sigma-Aldrich) were used and the experiments were performed within a few minutes after addition of the inhibitor, when cells had stopped contracting.

We thank Petri Auvinen, Keith Kozminski, Shoichiro Ono and Maria Vartiainen for critical reading of the manuscript. Evelyne and Jean-Claude Perriard, and Krzysztof Maruszewski are acknowledged for advice on isolation and culture of cardiomyocytes and for statistical analyses. Kimmo Tanhuanpää and Mika Molin are acknowledged for their expertise using light microscopy and Martin Bähler for GFP–β-actin and mCherry–β-actin constructs. Carol C. Gregorio is acknowledged for the generous gift of anti-tropomodulin antibodies. This study was supported by the Academy of Finland and Sigrid Juselius foundation. Aneta Skwarek-Maruszewska is a student of the Viikki Graduate School in Biosciences.

References

Agrawal, P. B., Greenleaf, R. S., Tomczak, K. K., Lehtokari, V. L., Wallgren-Pettersson, C., Wallefeld, W., Laing, N. G., Darras, B. T., Maciver, S. K., Dormitzer, P. R. et al. (2007). Nemaline myopathy with minicores caused by mutation of the CFL2 gene encoding the skeletal muscle actin-binding protein, cofilin-2. *Am. J. Hum. Genet.* **80**, 162-167.

Ayscough, K., Stryker, J., Pokala, N., Sanders, M., Crews, P. and Drubin, D. (1997). High rates of actin filament turnover in budding yeast and roles for actin in establishment and maintenance of cell polarity revealed using the actin inhibitor latrunculin-A. *J. Cell Biol.* **137**, 399-416.

Bai, J., Hartwig, J. H. and Perrimon, N. (2007). SALS, a WH2-domain-containing protein, promotes sarcomeric actin filament elongation from pointed ends during Drosophila muscle growth. *Dev. Cell* **13**, 828-842.

Bang, M. L., Li, X., Littlefield, R., Bremner, S., Thor, A., Knowlton, K. U., Lieber, R. L. and Chen, J. (2006). Nebulin-deficient mice exhibit shorter thin filament lengths and reduced contractile function in skeletal muscle. *J. Cell Biol.* **173**, 905-916.

Bertling, E., Hotulainen, P., Mattila, P. K., Matilainen, T., Salminen, M. and Lappalainen, P. (2004). Cyclase-associated protein 1 (CAP1) promotes cofilin-induced actin dynamics in mammalian nonmuscle cells. *Mol. Biol. Cell* **15**, 2324-2334.

Carlier, M. F., Laurent, V., Santolini, J., Melki, R., Didry, D., Xia, G. X., Hong, Y., Chua, N. H. and Pantaloni, D. (1997). Actin depolymerizing factor (ADF/cofilin) enhances the rate of filament turnover: implication in actin-based motility. *J. Cell Biol.* **136**, 1307-1322.

Casella, J. F., Craig, S., Maack, W. and Brown, A. E. (1987). Cap Z (36/32), a barbed end actin-capping protein, is a component of the Z-line of skeletal muscle. *J. Cell Biol.* **105**, 371-379.

Chaponnier, C. and Gabbiani, G. (2004). Pathological situations characterized by altered actin isoform expression. *J. Pathol.* **204**, 386-395.

Chereau, D., Boczkowska, M., Skwarek-Maruszewska, A., Fujiwara, I., Hayes, D. B., Rebowski, G., Lappalainen, P., Pollard, T. D. and Dominguez, R. (2008). Leiomodin is an actin nucleator in muscle cells. *Science* **320**, 239-243.

Chhabra, E. S. and Higgs, H. N. (2007). The many faces of actin: matching assembly factors with cellular structures. *Nat. Cell Biol.* **9**, 1110-1121.

Choidas, A., Jungbluth, A., Sechi, A., Murphy, J., Ullrich, A. and Marriott, G. (1998). The suitability and application of a GFP-actin fusion protein for long-term imaging of the organization and dynamics of the cytoskeleton in mammalian cells. *Eur. J. Cell Biol.* **77**, 81-90.

Colicos, M. A., Collins, B. E., Sailor, M. J. and Goda, Y. (2001). Remodeling of synaptic actin induced by photoconductive stimulation. *Cell* **107**, 605-616.

Coue, M., Brenner, S. L., Spector, I. and Korn, E. D. (1987). Inhibition of actin polymerization by latrunculin A. *FEBS Lett.* **213**, 316-318.

Fujita, H., Nedachi, T. and Kanzaki, M. (2007). Accelerated *de novo* sarcomere assembly by electric pulse stimulation in C2C12 myotubes. *Exp. Cell Res.* **313**, 1853-1865.

Gregorio, C. C., Weber, A., Bondad, M., Pennise, C. R. and Fowler, V. M. (1995). Requirement of pointed-end capping by tropomodulin to maintain actin filament length in embryonic chick cardiac myocytes. *Nature* **377**, 83-86.

Guettler, S., Vartiainen, M. K., Miralles, F., Larijani, B. and Treisman, R. (2008). RPEL motifs link the serum response factor cofactor MAL but not myocardin to Rho signaling via actin binding. *Mol. Cell. Biol.* **28**, 732-742.

Guha, M., Zhou, M. and Wang, Y. L. (2005). Cortical actin turnover during cytokinesis requires myosin II. *Curr. Biol.* **15**, 732-736.

Hasebe-Kishi, F. and Shimada, Y. (2000). Dynamics of actin and alpha-actinin in nascent myofibrils and stress fibers. *J. Muscle Res. Cell Motil.* **21**, 717-724.

Haviv, L., Gillo, D., Backouche, F. and Bernheim-Groswasser, A. (2008). A cytoskeletal demolition worker: myosin II acts as an actin depolymerization agent. *J. Mol. Biol.* **375**, 325-330.

Hotulainen, P. and Lappalainen, P. (2006). Stress fibers are generated by two distinct actin assembly mechanisms in motile cells. *J. Cell Biol.* **173**, 383-394.

Hotulainen, P., Paunola, E., Vartiainen, M. K. and Lappalainen, P. (2005). Actin-depolymerizing factor and cofilin-1 play overlapping roles in promoting rapid F-actin depolymerization in mammalian nonmuscle cells. *Mol. Biol. Cell* **16**, 649-664.

Kagawa, M., Sato, N. and Obinata, T. (2006). Effects of BTS (N-benzyl-p-toluene sulphonamide), an inhibitor for myosin-actin interaction, on myofibrillogenesis in skeletal muscle cells in culture. *Zool. Sci.* **11**, 969-975.

Kaksonen, M., Toret, C. P. and Drubin, D. G. (2006). Harnessing actin dynamics for clathrin-mediated endocytosis. *Nat. Rev. Mol. Cell. Biol.* **7**, 404-414.

Koestler, S. A., Auinger, S., Vinzenz, M., Rottner, K. and Small, J. V. (2008). Differentially oriented populations of actin filaments generated in lamellipodia collaborate in pushing and pausing at the cell front. *Nat. Cell Biol.* **10**, 306-313.

Kolega, J. (2004). Phototoxicity and photoinactivation of blebbistatin in UV and visible light. *Biochem. Biophys. Res. Commun.* **320**, 1020-1025.

Lappalainen, P. and Drubin, D. G. (1997). Cofilin promotes rapid actin filament turnover *in vivo*. *Nature*. **388**, 78-82.

Littlefield, R., Almenar-Queralt, A. and Fowler, V. M. (2001). Actin dynamics at pointed ends regulates thin filament length in striated muscle. *Nat. Cell Biol*. **3**, 544-551.

McElhinny, A. S., Schwach, C., Valichnac, M., Mount-Patrick, S. and Gregorio, C. C. (2005). Nebulin regulates the assembly and lengths of the thin filaments in striated muscle. *J. Cell Biol*. **170**, 947-957.

Medeiros, N. A., Burnette, D. T. and Forscher, P. (2006). Myosin II functions in actin-bundle turnover in neuronal growth cones. *Nat. Cell Biol.* **8**, 215-226.

Murthy, K. and Wadsworth, P. (2005). Myosin-II-dependent localization and dynamics of F-actin during cytokinesis. *Curr. Biol*. **15**, 724-731.

Okreglak, V. and Drubin, D. G. (2007). Cofilin recruitment and function during actin-mediated endocytosis dictated by actin nucleotide state. *J. Cell Biol.* **178**, 1251-1264.

Ono, S., Minami, N., Abe, H. and Obinata, T. (1994). Characterization of a novel cofilin isoform that is predominantly expressed in mammalian skeletal muscle. *J. Biol. Chem*. **269**, 15280-15286.

Ono, S., Baillie, D. L. and Benian, G. M. (1999). UNC-60B, an ADF/cofilin family protein, is required for proper assembly of actin into myofibrils in Caenorhabditis elegans body wall muscle. *J. Cell Biol*. **145**, 491-502.

Paavilainen, V. O., Bertling, E., Falck, S. and Lappalainen, P. (2004). Regulation of cytoskeletal dynamics by actin-monomer-binding proteins. *Trends Cell Biol.* **14**, 386-394.

Pantaloni, D., Le Clainche, C. and Carlier, M. F. (2001). Mechanism of actin-based motility. *Science* **292**, 1502-1506.

Pappas, C. T., Bhattacharya, N., Cooper, J. A. and Gregorio, C. C. (2008). Nebulin interacts with CapZ and regulates thin filament architecture within the Z-disc. *Mol. Biol. Cell* **19**, 1837-1847.

Pollard, T. D. and Borisy, G. G. (2003). Cellular motility driven by assembly and disassembly of actin filaments. *Cell* **112**, 453-465.

Rzadzinska, A. K., Schneider, M. E., Davies, C., Riordan, G. P. and Kachar, B. (2004). An actin molecular treadmill and myosins maintain stereocilia functional architecture and self-renewal. *J. Cell Biol.* **164**, 887-897.

Sanger, J. W., Kang, S., Siebrands, C. C., Freeman, N., Du, A., Wang, J., Stout, A. L. and Sanger, J. M. (2005). How to build a myofibril. *J. Muscle Res. Cell Motil.* **26**, 343-354.

Schafer, D., Hug, A. and Cooper, J. (1995). Inhibition of CapZ during myofibrillogenesis alters assembly of actin filaments. *J. Cell Biol.* **128**, 61-70.

Schratt, G., Philippar, U., Berger, J., Schwarz, H., Heidenreich, O. and Nordheim, A. (2002). Serum response factor is crucial for actin cytoskeletal organization and focal adhesion assembly in embryonic stem cells. *J. Cell Biol.* **156**, 737-750.

Soeno, Y., Shimada, Y. and Obinata, T. (1999). BDM (2,3-butanedione monoxime), an inhibitor of myosin-actin interaction, suppresses myofibrillogenesis in skeletal muscle cells in culture. *Cell Tissue Res.* **295**, 307-316.

Straight, A. F., Cheung, A., Limouze, J., Chen, I., Westwood, N. J., Sellers, J. R. and Mitchison, T. J. (2003). Dissecting temporal and spatial control of cytokinesis with a myosin II Inhibitor. *Science* **299**, 1743-1747.

Suzuki, H., Komiyama, M., Konno, A. and Shimada, Y. (1998). Exchangeability of actin in cardiac myocytes and fibroblasts as determined by fluorescence photobleaching recovery. *Tissue Cell* **30**, 274-280.

Vartiainen, M., Ojala, P. J., Auvinen, P., Peranen, J. and Lappalainen, P. (2000). Mouse A6/twinfilin is an actin monomer-binding protein that localizes to the regions of rapid actin dynamics. *Mol. Cell. Biol*. **20**, 1772-1783.

Vartiainen, M. K., Mustonen, T., Mattila, P. K., Ojala, P. J., Thesleff, I., Partanen, J. and Lappalainen, P. (2002). The three mouse actin-depolymerizing factor/cofilins evolved to fulfill cell-type-specific requirements for actin dynamics. *Mol. Biol. Cell* **13**, 183-194.

Vartiainen, M. K., Guettler, S., Larijani, B. and Treisman, R. (2007). Nuclear actin regulates dynamic subcellular localization and activity of the SRF cofactor MAL. *Science* **316**, 1749-1752.

Vignjevic, D., Kojima, S., Aratyn, Y., Danciu, O., Svitkina, T. and Borisy, G. G. (2006). Role of fascin in filopodial protrusion. *J. Cell Biol*. **174**, 863-875.

Wang, J., Shaner, N., Mittal, B., Zhou, Q., Chen, J., Sanger, J. M. and Sanger, J. W. (2005). Dynamics of Z-band based proteins in developing skeletal muscle cells. *Cell Motil. Cytoskeleton* **61**, 34-48.

Weber, A., Pennise, C. R., Babcock, G. G. and Fowler, V. M. (1994). Tropomodulin caps the pointed ends of actin filaments. *J. Cell Biol.* **127**, 1627-1635.

Witt, C. C., Burkart, C., Labeit, D., McNabb, M., Wu, Y., Granzier, H. and Labeit, S. (2006). Nebulin regulates thin filament length, contractility, and Z-disk structure *in vivo*. *EMBO J.* **25**, 3843-3855.

Yamashiro, S., Cox, E. A., Baillie, D. L., Hardin, J. D. and Ono, S. (2008). Sarcomeric actin organization is synergistically promoted by tropomodulin, ADF/cofilin, AIP1 and profilin in C. elegans. *J. Cell Sci.* **121**, 3867-3877.

Yarrow, J. C., Lechler, T., Li, R. and Mitchison, T. J. (2003). Rapid de-localization of actin leading edge components with BDM treatment. *BMC Cell Biol.* **4**, 5.